Damage Index of Steel Members under Severe Cyclic Loading

Yeon-soo Park[†], Suk-yeol Han[2], Byoung-chal Suh[2], Dong-ho Jeon[2], and Sun-joon Park[1]

[†]Department of Civil Engineering, Chonnam National University, Gwang-ju, Korea
[1]Department of Civil Engineering, Dongshin University, Naju, Chonnam, Korea
[2]Department of Civil Engineering, Chonnam National University, Gwang-ju, Korea

ABSTRACT

This paper aims at investigating the damage process of steel members leading to the failure under strong repeated loading, proposing the damage index using various factors related to the damage, and developing the analysis method for evaluating the damage state. Cantilever-type steel members were analyzed under uniaxial load and combined with a constant axial load, considering a horizontal displacement history. In analyzing the models, loading patterns and steel types (SS400, SM570, Posten80) were considered as main parameters. From the analysis results, the effects of parameter on the failures mode, the deformation capacity, the damage process are also discussed. Each failure process was compared as steel types. Consequently, the failure of steel members under strong repeated loading was determined by loading. Especially it was seen that the state of the failure is closely related to the local strain.

Keywords: damage index, local stress, local strain, plastic strain, repeated loading, failure mode

1. Introduction

There are many experiments and numerical analyses evaluating aseismatic damage on steel member such as columns, beams and bracings which are used as structure under cyclic loading such as the earthquake loading (Ge, 1996; Park, 1993; Gao, 2000). From this research, it is observed that total buckling is preceeded by local buckling, and the process of damage is the main cause of member fracture. The elements of a structure also undergo plastic deformation. In this case, though the repeat loading number is small, if the plastic deformation is large enough, the structure can fail. In the domain of several plastic deformations, therefore, a single member can be responsible for large damage to fracture through multiple plastic deformation.

As the collapse form of a steel member, there is the in-plane instability by deflection and transverse by a lateral buckling or a local buckling of a plate element. Among these, a member having a small slenderness ratio receives

† Corresponding author
Tel: +82-62-530-1657, Fax: +82-62-530-1659
E-mail address: parkys@chonnam.ac.kr

little effect from additional deflection by an axis force. A lateral buckling is caused by a local buckling, so the state of a local buckling in a plate element becomes the principal reason for collapse of steel members. Also, the form of fracture and damage in steel members changes with the mechanical factor such as stress and strain, the chemical factor of corrosion, and the properties of materials used(Crisfield, 1997).

The purpose of this study is to examine the damage process leading to failure caused by steel member undergoing plastic deformation, to obtain the basic data for the damage estimate, to deduce the most probable cause of damage and failure, and to suggest a new damage index by analyzing the fixed quantity of a factor. And by using the proposed damage index, the study is to develop damage analysis technique for box-style steel members.

2. Damage Evaluation

Recently, attempts to understand the nonlinear behavior of existing steel structures without applying the aseismatic detail and to estimate the aseismatic capacity have been made with the damage index which is used as a scale in order to understand the degree of damage. As a convenient

way to estimate the degree of damage in a structure and a member, the damage index expresses numerically the degree of damage of a structure and a member caused by loading and the capacity of a member. Such a damage index is classified into that of a structure and that of a member. For the structure, an estimating technique using the eigen period of a structure is applied, and for the member there is a technique using the change of stiffness, a fatigue formula, an energy emission history curve, and the change in strain.

2.1. Damage Index of a Member

In this study, damage is defined as the history process of deformation from the start of residue deformation to the start of failure. Under serious cyclic loading, the damage index in steel structure members is newly computed by study using the deformation access method(Park, 1993). The suggested damage index is very efficient because the damage of a member is estimated quantitatively by using the change of plastic strain in the plastic domain under heavy loading. In addition, the plastic strains of a tension domain and a compression domain are accessed separately, so the process of damage can be evaluated clearly. The study interprets the character of material in a plastic domain as bilinear kinematic hardening(Crisfield, 1997). Therefore, the relationship of stress-strain in the plastic domain can be expressed in not exponential form but in linear form, allowing one to easily grasp the degree of damage.

The damage index is calculated as follows. In the case of the steel member under heavy cyclic loading in the Fig. 1, the local stress-strain history curve of the weakest factor is drawn. In this history curve, the envelope curve of a stress ratio-strain ratio is drawn by using a yield stress and a strain. The limit stress ratio is σ_u/σ_y and the limit strain

ratio is $\varepsilon_u/\varepsilon_y$. In this envelope curve, the capability of damage resistance can be evaluated as an area ratio consisting of a stress ratio and a strain ratio corresponding to the cumulative plastic strain of the loading level and the limit loading state.

The upper contents are expressed as the damage index of Eq. (1).

$$D = \frac{1}{\alpha}\left(\frac{A^t_*}{A^t_{lim\ it}} + \frac{A^c_*}{A^c_{lim\ it}}\right) \tag{1}$$

$$\text{Here,}\quad A^t_* = \int_1^{\sigma^t_*/\sigma^t_y} \frac{(\varepsilon^t_*/\varepsilon^t_y - 1)}{(\sigma^t_*/\sigma^t_y - 1)}\frac{\sigma^t_*}{\sigma^t_y} d\left(\frac{\sigma^t_*}{\sigma^t_y}\right) \tag{1a}$$

$$A^c_* = \int_1^{\sigma^c_*/\sigma^c_y} \frac{(\varepsilon^c_*/\varepsilon^c_y - 1)}{(\sigma^c_*/\sigma^c_y - 1)}\frac{\sigma^c_*}{\sigma^c_y} d\left(\frac{\sigma^c_*}{\sigma^c_y}\right) \tag{1b}$$

$$A^t_{lim\ it} = \frac{1}{2}\left(\frac{\sigma^t_u}{\sigma^t_y} - 1\right)\left(\frac{\varepsilon^t_u}{\varepsilon^t_y} - 1\right) \tag{1c}$$

$$A^c_{lim\ it} = \frac{1}{2}\left(\frac{\sigma^c_u}{\sigma^c_y} - 1\right)\left(\frac{\varepsilon^c_u}{\varepsilon^c_y} - 1\right) \tag{1d}$$

Here, D is the damage index, A_* the area of plastic strain of a local stress ratio-strain ratio envelope curve in the loading level, $A_{lim\ it}$ the limit area of the plastic strain of a local stress ratio-strain ratio envelope curve, α as a strain constant take a value of 2 when it indicates a tension and a compression strain, and take a value of 1 when indicating a tension or a compression strain, σ_* a local strain in the loading level, ε_y a local stress in the loading level, σ_y a yield strain, σ_u a yield stress, n a limit strain, K a limit stress, n a strain-hardening modulus, K a strength exponent and superscript t and c tension and compression respectively.

The value of A_{limit} refers the area of a plastic strain in an envelope curve when a strain approaches to a limit strain under the most intense stress intensity. When $D=1$, a member starts failure in the corresponding loading level and when $D<1$, it shows numerically how much damage occurs before reaching the state of failure.

Generally, the exact estimate of the history of a local strain is made possible by finite element analysis and an experiment regarded with material or geometric nonlinear. In result, the plastic strain and A_{limit} is presented with respect to the steel type using the program, Sol.106 of MSC/NASTRAN Version 70. 7. 2.
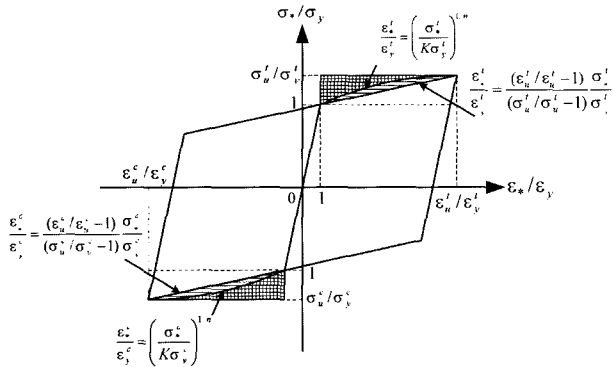

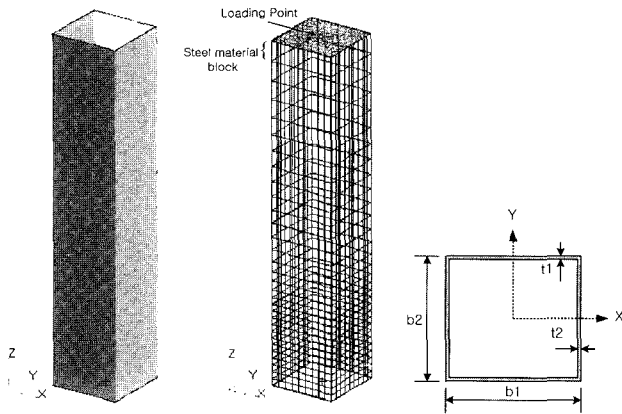**Fig. 1.** Envelope curve of dimensionless local stress ratio-strain ratio

Fig. 2. Analysis modeling of a box-styled steel member

3. Finite Element Analysis for the Evaluation of Damage

3.1 Nonlinear Analysis Modeling

To develop an analysis technique for the damage index suggested in this study for steel members under heavy loading, material and geometric nonlinear analysis is conducted using a box-styled steel member.

Fig. 2 shows the finite element model and basic coordinates of a box-styled steel member. In an analysis model, a box steel B-100 × 100 × 2.3 is used. The model consists of a fixed edge and a far hinge edge rotating freely around a Y axis which moves through the upper and lower section, with the length h of both sections being 480 mm.

In a structure model, the four side factor (QUAD4) of a shell plate isoparmetric element is used and the triangle element (TRIA3) is used near the member edge part of the loading point. In the QUAD4, the curvature is supposed to undergo linear transformation and in the TRIA3, the strain and the curvature are to be constant(MSC/NASTRAN, 1992). For the model of this analysis, a 1116 element model is divided into 31 partitions in the direction of local axis and into 9 partitions perpendicular to the local axis (4 sides total). The element partition of these models is made by considering not only the state of member deformation such as whole buckling and local buckling, but also location such as local strain.

Each node displacement has 6 degrees of freedom in the general three-dimensional analysis, but this analysis has only 5 degrees of freedom for rotation around a tangent line of a plate element when using a rotation constraint in which stiffness has not been defined. In the model of Fig. 1, part of a steel block is forced to behave like a rigid body by enlarging the elastic coefficient and yield strength. Each name and dimension of the model is shown in Table 1.

Table 1. Name and dimension of a model

Length h(mm)	Width $b1$(mm)	Width $b2$(mm)	Thickness t(mm)
480	100	100	3.2

Section area A(mm²)	Rotation radius r(mm)	Width-thickness ratio b/t	Slenderness ratio λ
1239.04	39.54	29.25	24.28
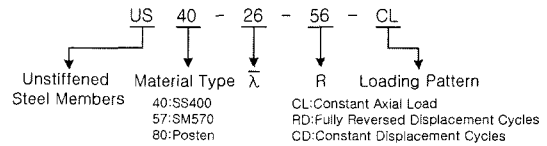
$\bar{\lambda}$ is the slenderness ratio parameter of a compression member.

$$\bar{\lambda} = \frac{1}{\pi}\frac{\sqrt{\sigma_y}}{E}\left(\frac{l_e}{r}\right) \qquad (2)$$

Here, E is Young's modulus, l_e the length of an effective buckling(=Kl, K is the effective buckling length modulus (K in compression member of the fixed edge is 2.0)) and r the rotation radius. R is the equivalent width-thickness ratio parameter of a plate.

$$R = \frac{1}{\pi}\left(\frac{b}{t}\right)\frac{\sqrt{12(1-v^2)}}{k}\sqrt{\frac{F_y}{E}} \qquad (3)$$

Likewise, t is the thickness of a plate, b the width and k the buckling coefficient (k for a compression member of the simple 4 sides support is 4).

3.2 Establishment of Loading Method

First, the analysis on the compression member receiving a center axis load is conducted. Then, with the compression force of 0.2 P_y imposed in the point of loading, the relative displacement is set according to the level in a direction perpendicular(an X axis) to a local axis of Fig.2. Here, displacement, strain, load, or stress set the direction of a compression as positive. The repetition loading pattern has two kinds as shown in Fig. 3: (a) an alternating increasing(two times as much as the yield horizontal displacement) displacement loading which is RD(Fully Reversed Displacement Cycles) type in the tension-compression domain, and (b) an alternating fixed(three times as much as the yield horizontal displacement) displacement loading which is CD (Constant Displacement Cycles) type in the tension domain. The yield horizontal displacement is cal-
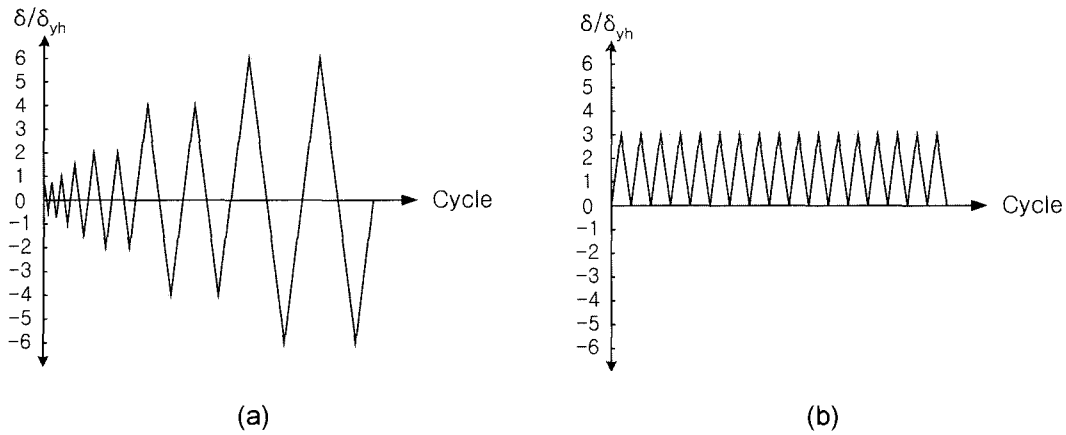
(a)

(b)

Fig. 3. Loading pattern

culated from the next Eq. (4).

$$\delta_{yh} = \frac{P_{yh}h^3}{3EI} \tag{4}$$

Here,

$$P_{yh} = \frac{M_y}{h} \tag{4-1}$$

Here, M_y is yield moment and P_{yh} yield horizontal load.

3.3 Assumption of Material Property

In order to describe material properties, the bilinear stress-strain relation of movement hardness shown in Fig. 4 is used. Table 2 shows the relationship between a slope E_t and Young's modulus E of a single axis stress-strain curve on the plastic domain, a nominal yield stress, Young's modulus and poisson's ratio v. The yield condition of Von Mises is also used.

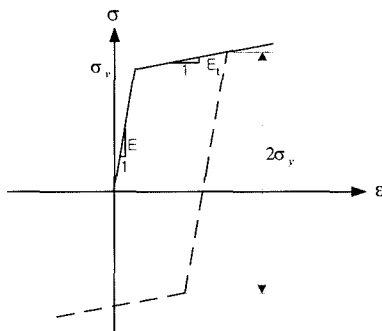Generally, the accuracy of a member history behavior

Fig. 4. A stress-strain relation supposed in the elastic-plastic material

Table 2. Material properties

Specimen	σ_y (MPa)	σ_u (MPa)	E_t / E	Material Type
US40-*	235.2	510	24	SS400
US57-*	460.6	597	15	SM570
US80-*	686.0	821	10	Posten80

Note: E=205Gpa, v=0.3, *=All inclusion of attached name

analysis is affected by the material composition. The analysis of the strain hardness domain requires the accurate modeling of material composition. As this study is about the relationship of the repetition stress-strain of a steel material in the strain domain, it uses the connection of the material composition of the bilinear stress-strain to develop an analysis technique applying the damage index. For more accurate analysis, a modeling of history composition including isotropic hardening is regarded to be needed.

3.4 Variables used in the Analysis

In this study an analysis carried out with steel type and the loading conditions. The steel types are applied to a general structure type-rolled steel material SS 400, a weld structure type-rolled steel material SM 570 and a high-tensile steel material Posten 80.

Loading conditions are as follows; 1. A CL(Constant Axial Load) type under a center axis compression load 2. An alternating steady increase displacement RD type of a tension-compression domain in the state of a center axis compression load $0.2P_y$ 3. An alternating fixed displacement RD type of a tension domain in the state of a center axis compression load $0.2P_y$ The process of damage and the behavior of failure are compared and analyzed by conducting nonlinear analysis according to each loading con-

Table 3. Variables used in the analysis

Specimen	Material Type	Loading Pattern
US-40-26-56-CL	SS400	CL
US-40-26-56-RD	SS400	RD
US-40-26-56-CD	SS400	CD
US-57-26-56-CL	SM570	CL
US-57-26-56-RD	SM570	RD
US-57-26-56-CD	SM570	CD
US-80-45-95-CL	Posten80	CL
US-80-45-95-RD	Posten80	RD
US-80-45-95-CD	Posten80	CD

dition. These results are shown in Table 3.

4. Results and Discussions

4.1. Steel Material under Center Axis Load

After a steel member under the center axis load reaches its maximum strength, the buckling strength falls suddenly. As the box typed steel member has no distinction of a strong axis and a weak axis and four sides are welded, the effect of compression residue stress is very high.

The location of a local buckling deformation is $0.146h$ in US40-26-56-CL specimen, $0.125h$ in US57-36-78-CL and $0.114h$ in the center part on the opposite plane of the buckling direction in US80-45-95-CL. This shows that as the strength of a steel material gets stronger, the location of a local buckling deformation gets lower. The analytical results of center compression are shown in Table 4. This table shows the strength and stress size of each specimen.

The plastic strain width is similar in both the US57-36-78-CL and US80-45-95-CL specimens but is 2.53 times

this amount in US40-26-56-CL. Local stress-stain history is shown in Fig. 5.

4.2. Steel Member under the alternating Displacement

4.2.1. Member Deformation and Figure of Failure

As the alternating increase displacement(RD) in the tension-compression domain is applied toward the direction of the members +X axis, the location of local buckling is generated near both corner parts on a +X plane about $0.04h$ above a fixed edge regardless of steel type. This explains why the energy dispersion effect and the buckling strength drop sharply due to the repeated deformation in the corner part of a strong stiffness with concentrated residual stress.

Fig. 6 shows the shape of deformation when the loaded repeat displacement is 0 just before specimen failure. In all specimens, there is a local buckling which is followed by a whole buckling. The shape of the buckling is not generated over the whole length of all specimens but creates a continuous deformation from the part in which buckling happens first. The section shows the bending of a half wave type. As load is increased to yield strength only a compression deformation occurs and as load exceeds yield strength whole buckling happens. According to the increase of a load, local buckling is generated. The deformation shape according to specimen and load conditions is shown in Fig. 6.

4.2.2. Local Stress-Strain History

Fig. 7 shows a local stress-strain relationship. This stress-strain history shows the condition of a deflection tension and a deflection compression about a corner element around an edge in which a local buckling deformation
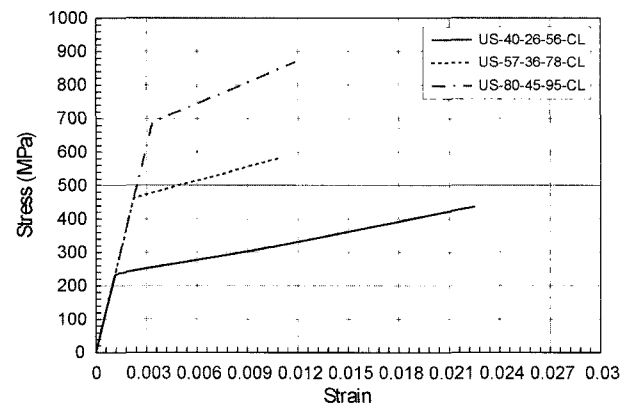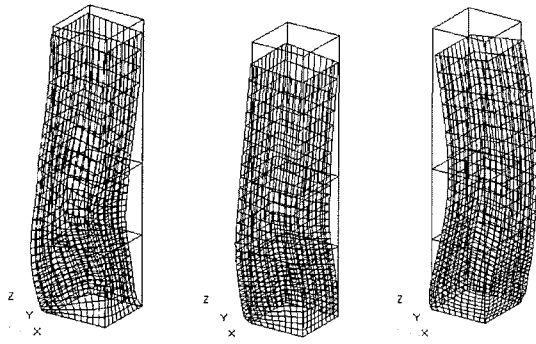
Table 4. Results of center compression analysis

US40-26-56-CL			
Maximun Strength P_u(KN)	Yield Strength P_y(KN)	Maximun Stress σ_{ut}(Mpa)	Yield Stress σ_{yt}(MPa)
409.32	303.13	437.12	237.16
US57-36-78-CL			
Maximun Strength P_u(KN)	Yield Strength P_y(KN)	Maximun Stress σ_{ut}(Mpa)	Yield Stress σ_{yt}(MPa)
726.59	578.79	577.22	460.00
US80-45-95-CL			
Maximun Strength P_u(KN)	Yield Strength P_y(KN)	Maximun Stress σ_{ut}(Mpa)	Yield Stress σ_{yt}(MPa)
927.80	853.47	926.85	686.00

Fig. 5. Local stress-strain curves according to specimen and loading condition(CL)

(a)US40-26-56-RD (b)US40-26-56-CD (c)US57-36-78-RD
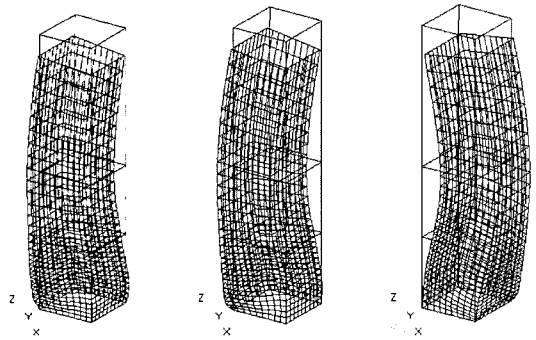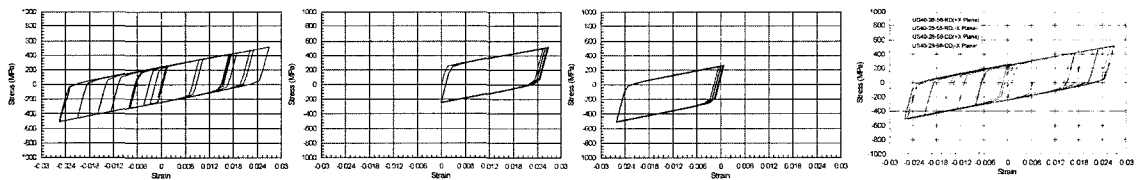

(d)US57-36-78-CD (e)US80-45-95-RD (f)US80-45-95-CD

Fig. 6. Deformation figure according to specimen and load conditions(RD, CD)

occurs. In each figure, (a) is a history curve about a +X plane of the load condition RD type according to steel type, (b) is a history curve about a +X plane of the load condition CD type according to steel type, and (c) is a history curve combining both a +X plane and a -X of the load condition RD type and the CD according to steel type.

In figure (a), in the case of the US40-26-56-RD specimen, the amplitude difference of tension strain in a compression strain is 1.49 ε_y. The recovery of tension strain for a compression strain is 93.7%. In the case of the US57-36-78-RD specimen, the amplitude difference of tension strain in a compression strain is 1.71 ε_y. Likewise tension strain recovery for a compression strain is 69.6%. In the case of the US80-45-95-RD specimen, the amplitude difference of tension strain in a compression strain is 2.24 ε_y. Likewise tension strain recovery for a compression strain is 50.2%.

Regarding the amplitude difference, the US57-36-78-RD specimen is increased 1.15 times more than the US40-26-56-RD specimen and 1.51 times more than the US80-45-95-RD specimen. This local strain history indicates that the condition of deflection compression is very serious. the steel material with more strength undergoes more serious compression strain. It is conjectured that the compression part having a large strain cracks first, and the tension part.
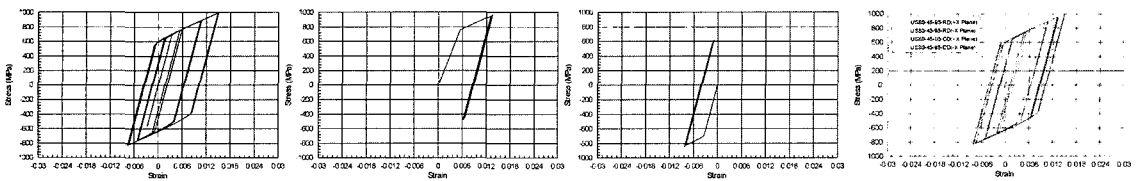
The strain recovery ability of the US57-36-78-RD specimen is 74.3% lower than that of the US40-26-56-RD specimen and the US80-45-95-RD specimen 53.6% lower

(a-1)US40-26-56-RD(+X Plane) (b-1)US40-26-56-CD(+X Plane) (b-4)US40-26-56-CD(-X Plane) (c-1) US40-26-56
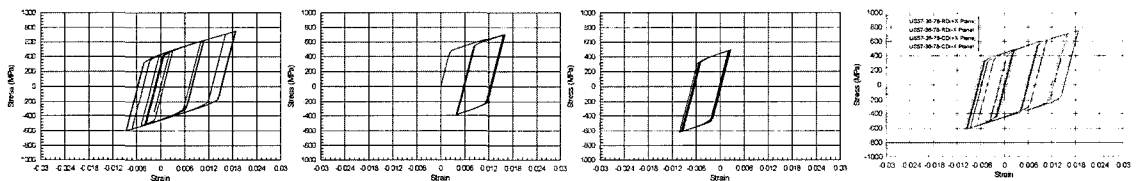
(a-2)US57-36-78-RD(+X Plane) (b-2)US57-36-78-CD(+X Plane) (b-5)US57-36-78-CD(-X Plane) (c-2) US57-36-78

(a-3)US80-45-95-RD(+X Plane) (b-3)US80-45-95-CD(+X Plane) (b-6)US80-45-95-CD(-X Plane) (c- 3) US80-45-95

Fig. 7. Local stress-strain curves according to specimen and loading conditions(RD, CD)

han that of. the US40-26-56-RD specimen.

In figure (b), according to the load condition, compression strain happens on a +X plane and tension strain and compression strain on a -X plane. Because it is under the load of a center axis, a compression strain is also on a -X plane. The recovery ability on a +X plane is as follows: US40-26-56-RD specimen 98%, US57-36-78-RD 76.5% and US80-45-95 52%.

Regard the strain recovery ability, the US57-36-78-RD specimen shows a 53% decrease than the US40-26-56-RD specimen. In a strong steel material which reaches its limit strain, the plastic strain width decreases sharply according to load period. Fig. 8 (a), (b) and (c) show member stress

Table 5. Limit area of a local stress ratio-strain ratio envelope curve according to specimen

	US40-26-56	US57-36-78	US80-45-95
$A^t_{lim\,it}$	24.87	0.87	0.35
$A^c_{lim\,it}$	27.30	2.91	1.57

distribution according to specimen.

4.3. Damage Evaluation Using the Damage Index

The limit area of the plastic strain of a stress ratio-strain ratio envelope curve(Fig. 9) according to specimen is summarized in Table 5. The envelope curve of a local stress ratio-strain ratio history curve on a section having a serious stress intensity for a load condition of CL type, RD and CD is drawn. These are the values obtained through the conditions in which the envelope curve is made dimensionless and applied to the box typed steel member as specified in chapter 2.1.

The limit area can be used to determine the degree of damage of a box type steel member. Fig. 10 shows the damage index distribution of the compression domain of a plane according to the loading condition RD. The corner part near an edge has the most serious degree of damage. And in the case of a specimen with a low strength, the area of damage is centered near an edge. In the case of the US40-26-56-RD specimen, there is nearly no damage in
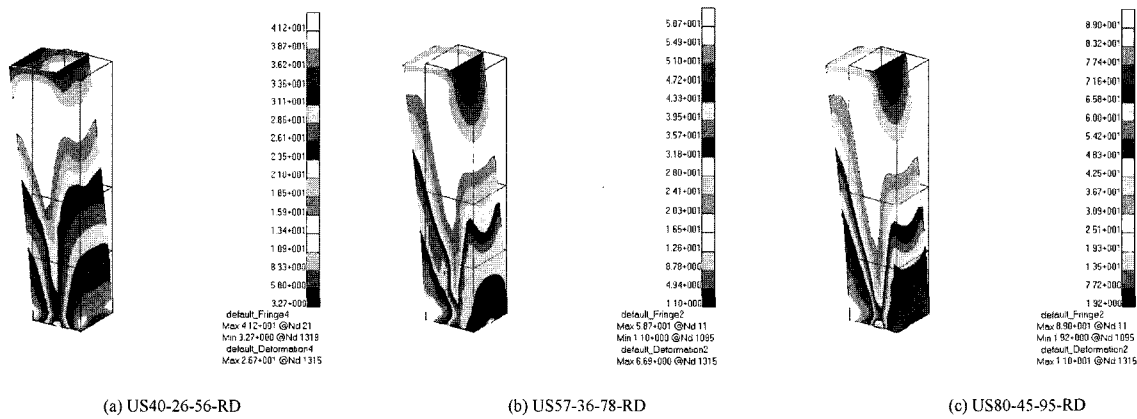

(a) US40-26-56-RD   (b) US57-36-78-RD   (c) US80-45-95-RD

Fig. 8. Stress distribution according to specimen (kgf/mm²)
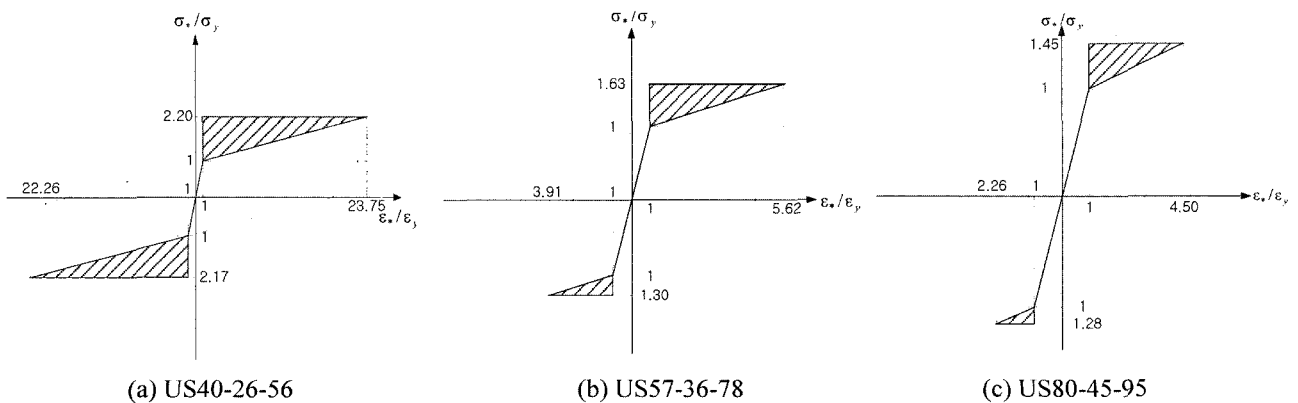
(a) US40-26-56   (b) US57-36-78   (c) US80-45-95

Fig. 9. Dimensionless local stress ratio-strain ratio envelope curve according to specimen

(a-1) US40-26-56-RD(+X Plane)   (a-2) US57-36-78-RD(+X Plane)   (a-3) US80-45-95-RD(+X Plane)

(b-1) US40-26-56-RD(-X Plane)   (b-2) US57-36-78-RD(-X Plane)   (b-3) US80-45-95-RD(-X Plane)

Fig. 10. Compression domain damage index distribution on a plane according to specimen or load condition RD

(a-1) US40-26-56-RD(+X Plane)   (a-2) US57-36-78-RD(+X Plane)   (a-3) US80-45-95-RD(+X Plane)

(b-1) US40-26-56-RD(-X Plane)   (b-2) US57-36-78-RD(-X Plane)   (b-3) US80-45-95-RD(-X Plane)
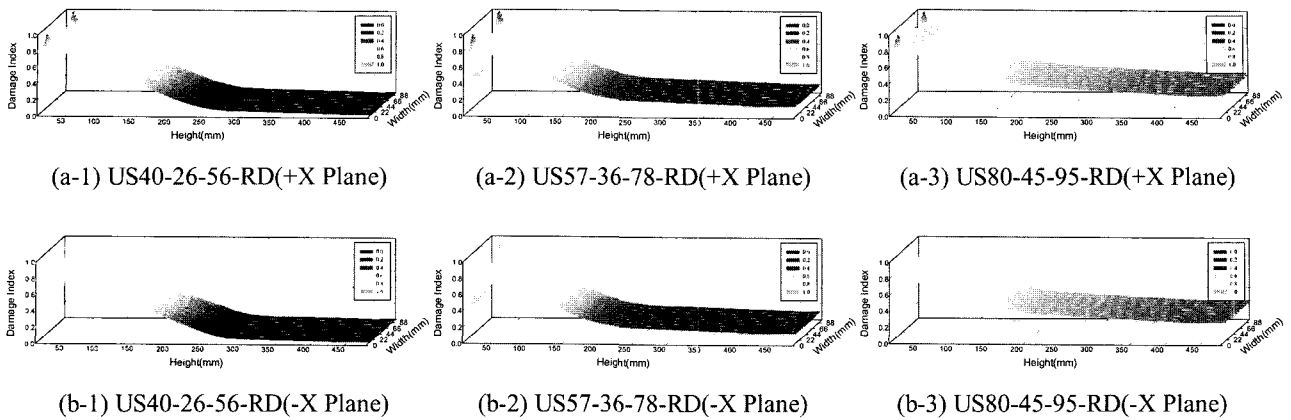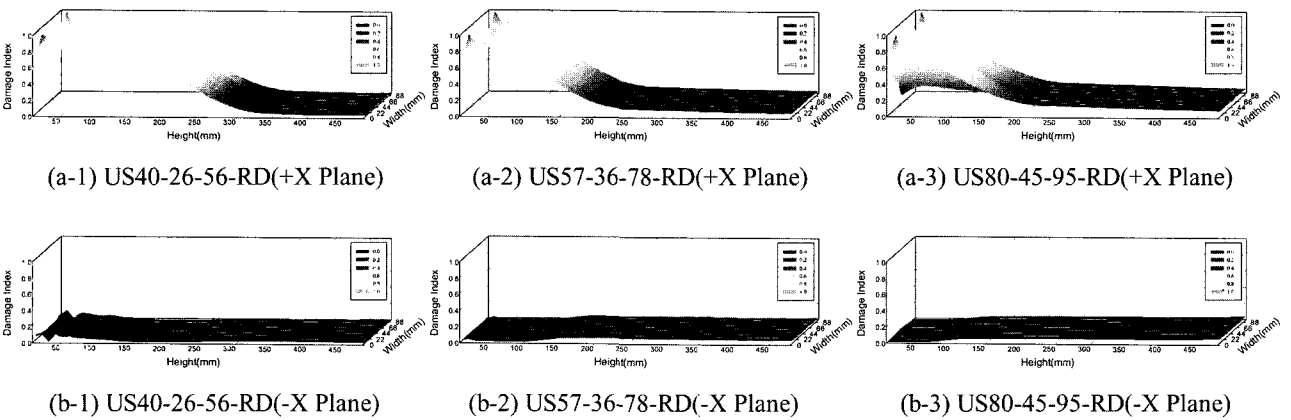
Fig. 11. Compression domain damage index distribution on a plane according to specimen or load condition RD

the area above $0.5h$.

A specimen having great strength shows even damage distribution over the height of a steel member. US80-45-95-RD has the damage index over 0.4 to member height.

The Fig. 11 shows the damage index distribution of the compression domain of a plane according to the load condition CD. Like the load condition RD, the degree of damage is intense in a corner near an edge. Contrary to the load condition RD, the area of damage in a specimen having a weak strength is bigger. US40-26-56-CD has a damage effect up to $0.63h$.

The area of damage in the case of a specimen having greater strength is limited to an edge. US80-45-95-RD has a damage effect approaching $0.35h$ of member height.

5. Conclusions

This study examines the damage process involved in the failure of a steel member undergoing the cyclic plastic deformation and accessed newly to the evaluation of the

degree of damage by using the elements related to damage and utilizes nonlinear analysis on the box type steel membe under a severe cyclic load in order to develope an analytica technique which evaluates the degree of damage.

(1) The new damage index formula is suggested by using the envelope curve of a dimensionless loca stress ratio-strain ratio. In the case of one under the cyclic load, the degree of damage is determined by considering a compression strain and a tension strain

(2) As the result of damage evaluation using the damage index of the box typed steel member, the severely damaged part is located in the area of local buck ling. This means that the damage is related to loca buckling and a plastic strain.

(3) In the case of local buckling imposed a center axi: load, as the strength of steel materials increases, the buckling location is lower. But under repeat load regardless of steel material strength buckling hap pens near an edge.

(4) Although the strength of a high-tensile steel Poster

80 steel member is 1.5 times higher than a SM570, the strain recovery ability of a Posten80 steel member doesn't fall lower than that of a SM570.

Acknowledgements

References

Bannantine JA, Comer JJ, Handrock JL (1990) Fundamentals of metal fatigue analysis, Prentice-Hall Inc.

Choi CG (1989) Finite element analysis, Jip Moon Dang.

Chopra AK (1995) Dynamics of structures theory and applications to earthquake engineering, Prentice Hall.

Crisfield MA (1997) Non-linear finite element analysis of solids and structures, Volume 1, John Wiley & Sons Ltd.

Crisfield MA (1997) Non-linear finite element analysis of solids and structures, Volume 2, John Wiley & Sons Ltd.

Gao S, Usami T (2000) Eccentrically loaded steel columns under cyclic in-plane loading, Journal of Structural Engineering/August 2000: 964-972.

Ge H (1996) Cyclic tests of concrete-filled steel box columns, Journal of Structural Engineeing ASCE/October 1996 : 1169-1177.

Jiang L, Goto Y, Obata M (2001) Multiple spring model for 3D-hysteretic behavior of thin-walled circular steel piers, Structural Eng./ Earthquake Eng. JSCE/Vol.18 No.2 : 111-127.

MSC/NASTRAN (1992) Nonlinear analysis, The Macneal-Schwendler Corporation.

Nomaka T, Iwai S (1998) Failure of bar structure under repeated loading, John & Sons.

Park YS (1993) Damage process of steel members under very-low-cycle loading, Dissertation of Civil Engineering Department, Kyoto Unibersity.

Park YS, Park SJ (1998) Quantitative damage model of steel member under strong seismic loading, Journal of Korea Society of Steel Construction 10(3) 339-353.

Park YS, Park SJ, Kang SH, Eun YF (1997) A study on plastic fatigue of steel structure element subjected to repeated loading, Journal of Korea Society of Steel Construction 9(2) 193-204.

Park YS (1997) A study on experimental and numerical analysis for structural failure identification of steel members under earthquake loading, Pohang Iron and Steel Co. 97KO29.